INSPECTION GUIDE FOR COLUMN SPLICE REGIONS AFFECTED BY PREMATURE CONCRETE DETERIORATION

by

Joseph M. Bracci
Research Engineer
Zachry Department of Civil Engineering and
Texas A&M Transportation Institute

Report 0-5722-P2
Project 0-5722
Project Title: Lap Splice and Development Length Performance in ASR and/or DEF Damaged Concrete Elements

Performed in cooperation with the
Texas Department of Transportation
and the
Federal Highway Administration

Published: July 2016

TEXAS A&M TRANSPORTATION INSTITUTE
College Station, Texas 77843-3135

DISCLAIMER

This research was performed in cooperation with the Texas Department of Transportation (TxDOT) and the Federal Highway Administration (FHWA). The contents of this report reflect the views of the author, who is responsible for the facts and the accuracy of the data presented herein. The contents do not necessarily reflect the official view or policies of the FHWA or TxDOT. This report does not constitute a standard, specification, or regulation. This report is not intended for construction, bidding, or permit purposes. The engineer in charge of the project was Joseph M. Bracci, P.E. #79855.

ACKNOWLEDGMENTS

This project was conducted at Texas A&M University and was supported by the Texas Department of Transportation and the Federal Highway Administration through the Texas A&M Transportation Institute. The author acknowledges the efforts and contributions of the TxDOT research project manager, Wade Odell, project director, Ricardo Gonzalez, and the members of the Project Monitoring Committee, including Keith Ramsay, Robert Owens, and John Vogel. The author would like to acknowledge the participation and contributions of Drs. David Trejo and Paolo Gardoni in this research program. The author is grateful and is especially proud of the graduate and undergraduate student researchers involved in the research program including Ryan Alberson, Kathleen Eck Olave, Jason Zidek, Marcus Schniers, and the many other students that contributed during the large-scale specimen construction. The author thanks Dr. Peter Keating and Mr. Matt Potter of the Civil Engineering High-Bay Structural and Materials Laboratory at Texas A&M University for their technical and logistical assistance during the construction and structural testing of the large-scale specimens. The author acknowledges the donation of reinforcing steel for the large-scale specimens from CMC Inc., in particular Paul Fredrickson.

TABLE OF CONTENTS

Page

LIST OF FIGURES

Page

LIST OF TABLES

Page

CHAPTER 1: PURPOSE AND SCOPE

1.1 PURPOSE

This guideline aims to help bridge inspectors and engineers in identifying and assessing the capability of reinforced concrete column splice regions affected by varying degrees of premature concrete deterioration due to alkali-silica reaction (ASR) and delayed ettringite formation (DEF). This guideline is a condensed version of the final project reports by Bracci et al. (2012) and Bracci (2014), and also papers by Eck Olave et al. (2014a, 2014b). The author strongly encourages interested readers to review the final project reports and papers for more details and further explanations.

1.2 SCOPE

This guideline begins by providing a brief overview of ASR and DEF, along with short summaries of the relevant literature from technical reports and journal publications. To assist bridge inspectors and engineers, some representative cracking observed in field structures throughout Texas is provided. Next, a summary of the experimental program performed as part of this research highlights the specimen exposure program (including concrete expansion and crack width measurements) and the results of the structural load testing of column splice specimens with varying degrees of primarily ASR deterioration. Findings and recommendations of the research are summarized at the end of the report.

CHAPTER 2: PREMATURE CONCRETE DETERIORATION DUE TO ASR/DEF

This chapter provides a brief overview of some of the mechanisms and effects of premature concrete deterioration due to ASR and/or DEF that are believed to cause cracking in various bridges across Texas.

2.1 OVERVIEW

Over the past 25 years or so, the Texas Department of Transportation (TxDOT) has had an aggressive construction program in place to accommodate the expanding population growth within Texas. A significant amount of construction has occurred throughout the state, especially in major metropolitan areas. Because of constrained conditions in metropolitan areas in terms of access space and the raw scale of transportation systems needed to satisfy the increasing traffic demands, the size of transportation structures, both at the member and system levels, have become significantly larger than past construction. Unlike nominal size concrete placements, large concrete placements can experience elevated temperatures during hydration, which can later cause cracking and deterioration of these concrete structures. Contractors have taken aggressive approaches in building such structures to meet the construction demands in these metropolitan areas. In addition to taking aggressive approaches in scheduling and in resource allocations, some contractors are believed to have proportioned concrete mixtures with early set cement (Type III) to achieve high early strengths. By doing so, contractors can remove forms more quickly, allowing the construction to be completed in an expedited fashion. Although this practice is advantageous in minimizing construction costs and build time, it may have contributed to the early cracking of many structures (termed *premature concrete deterioration*).

In addition, the chemical constituents in the cement and aggregates play a key role in the durability of concrete structures. Professor Folliard's research group at The University of Texas at Austin (Bauer et al. 2006; Folliard et al. 2006) has documented that high alkali contents in cement, especially in Type III cement, when used with reactive siliceous aggregates (which are prominent in Texas) in concrete in the presence of moisture can result in alkali-silica reaction. ASR can lead to the formation of expansive by-products, which in turn can lead to cracking of the concrete. Folliard et al. (2006) and Burgher et al. (2008) also found that concrete cracking from ASR can lead to other deterioration processes, such as delayed ettringite formation and corrosion, which can further reduce the capacity of the structure.

2.2 ALKALI-SILICA REACTION

ASR is the chemical reaction between the alkalis in concrete (generally from high alkali cement with alkali contents greater than about 5 lb/cy [3 kg/m^3]; Canadian Standards Association 2000) and reactive silica found in naturally occurring aggregates. Conditions required for ASR initiation and propagation include reactive silica phases in the aggregate, availability of alkali hydroxides in the pore solution ([Na^+], [K^+], or [OH^-]), and sufficient moisture (Folliard et al. 2006). The reaction between the reactive silica in the aggregate and the alkalis in the pore solution produce a product, commonly referred to as ASR gel, that expands throughout the concrete when exposed to additional moisture, causing overall concrete expansion. As with most chemical reactions in

semi-closed systems, the alkalis and reactive silica can be consumed with time, reducing the rate of expansion (Folliard et al. 2006).

Berube et al. (2002) reported that the exposure conditions of concrete members can influence ASR expansion and surface cracking development. In particular, in Berube et al.'s study, wetting and drying cycles of laboratory specimens greatly promoted surface cracking despite the fact that the surface expansion due to ASR was reduced.

Folliard et al. (2006) found that as ASR gel forms, tensile stresses develop internally in the concrete. In general, the hydrated cement paste (HCP) is weaker than the aggregates, and cracking initially occurs in the HCP or within the interfacial transition zone (Poole 1992; Swamy 1992). However, Jensen (2003) reported that ASR-damaged concrete can exhibit cracking in both the HCP and aggregates and quantified the amount of cracking in the aggregates. Aggregate cracking may influence the shear capacity (aggregate interlock) and may be a factor that influences the bond strength of reinforcement in concrete.

ASR-induced expansion of concrete can be significant. Fan and Hanson (1998b) measured length changes approaching 0.4 percent (strain of 0.004) in unreinforced concrete specimens subjected to accelerated exposure conditions. While these expansions may be significant, the presence of reinforcement can reduce the expansion and concrete cracking (Bae et al. 2007). Fan and Hanson (1998a, 1998b) measured a 50 percent reduction in the expansion of concrete when 0.54 percent steel reinforcement (greater than the minimum code requirements) was present in the element. However, Fan and Hanson (1998a and 1998b) reported that the ASR expansion can still be significant enough to yield the reinforcement.

2.3 DELAYED ETTRINGITE FORMATION

High cement contents in large-volume concrete structures can lead to significant heat generation during hydration, which potentially can lead to concrete cracking from both thermal stresses and later age reformation of ettringite within the concrete (referred to as delayed ettringite formation). Researchers, including Petrov et al. (2006) and Burgher et al. (2008), have developed hypotheses on how DEF occurs in hardened concrete. In general, ettringite forms at early ages in fresh concrete. As the sulfates in the cement react with the calcium aluminates in the presence of calcium hydroxide, the sulfates are consumed. Once the sulfate concentration in the pore solution reaches a lower value, the calcium aluminate reacts with the already-formed ettringite to produce monosulfoaluminate (Folliard et al. 2006). If sulfates are reintroduced to the pore solution, the monosulfoaluminates can revert to ettringite, causing overall concrete expansion. Ettringite reformation in hardened concrete is likely when the concrete curing temperatures exceed reported minimum values of 148 to 160°F (64 to 71°C; Hobbs 1999; Thomas 2001; Folliard et al. 2006; Petrov et al. 2006; Burgher et al. 2008).

DEF-induced expansion of concrete can greatly exceed that of ASR. Grattan-Bellew et al. (1998) measured a maximum expansion caused by DEF of greater than 0.4 percent over a period of about 65 days. Kelham (1996) found that after about 5 years of storage, DEF can cause expansions exceeding 2 percent. Unlike ASR, where the stresses and cracking typically initiate at the HCP-aggregate interface, internal stresses from DEF typically occur in the HCP at void locations (Burgher et al. 2008). Although damage initiates in different areas, both ASR and DEF

mechanisms lead to cracking of the HCP and, depending on the degree of expansion, later cracking of the aggregates. In addition, Folliard et al. (2006) reported that cracking due to ASR can occur first, and under certain conditions, DEF can follow.

Based on the research of Folliard et al. (2006) and Burgher et al. (2008), TxDOT developed and implemented guidelines for placing concrete (400 Items—Structures, in Standard Specifications for Construction and Maintenance of Highways, Streets, and Bridges) such that certain temperatures are not exceeded during concrete curing. In general, these guidelines have reduced the likelihood of DEF damage, but structures constructed prior to these guidelines can still be susceptible to DEF and cracking.

In bridge structures in Texas, DEF does not seem to be as prevalent as ASR. Structures for the most part have not been identified as exhibiting only DEF damage, with one possible exception in San Antonio. In general, it is thought that structures first exhibit cracking due to ASR and then exhibit DEF damage. Although ASR and DEF are different mechanisms of concrete deterioration, in general, both lead to volumetric expansion of concrete and eventual cracking of concrete usually in the tension field of the element from induced loading. It is this cracking that has the potential to reduce the capacity of structures and also lead to other durability issues.

2.4 ASR/DEF EFFECTS ON MATERIAL PROPERTIES AND STRUCTURAL PERFORMANCE

Bracci et al. (2012) highlighted the significant research in the literature on the impact of ASR and DEF on concrete material properties, such as the compressive strength, tensile strength, flexural strength, and modulus of elasticity of small-scale samples, and on structural properties, such as bending, bearing, shear, and bond strength. In general, most studies reveal that concrete properties can be reduced when internal expansive forces are present. The lack of research performed on the effects of internal expansion on the structural performance, especially in large-scale specimens, is particularly noteworthy for justifying the research presented here. Much of the data in the literature has focused on small-scale specimens, which likely do not have the same behavior as large-scale specimens for a variety of reasons including concrete surface-to-volume ratios that will impact total alkali content and reinforcement sizes and detailing.

2.5 ASR/DEF EFFECTS ON CONCRETE BRIDGE STRUCTURES IN TEXAS

Both ASR and DEF can lead to volumetric expansion of concrete; therefore, initial cracking from these mechanisms typically develops in the tension field of the concrete member under gravity loading. This research program investigated the structural performance of column specimens, with particular focus on the lap splice region, with varying levels of ASR and DEF. Figure 2-1 shows an example bridge column in Texas under predominantly concentric axial service loading where cracks have developed in the splice region (directly above the foundation), and these cracks were reported to be primarily due to ASR (Folliard et al. 2009). The figure shows that cracks propagate vertically along the column length in the direction of the tension field caused by Poisson's effect from the compressive axial service loads on the structure. For columns of cantilevered bents with applied overturning moments (see Figure 2-2), predominant cracking first develops in the tension field due to the overturning moment (Bracci et al. 2012).

However, in both cases, as ASR/DEF effects continue, cracks can also develop in other directions from the initial cracks that formed in the tension field (see Figures 2-1 and 2-2a). Shear cracking in the D-regions (bent cap-column joint regions) are also evident. Figure 2-3 shows an example of a bridge bent cap with mapped cracking predominantly influenced by ASR under minor levels of gravity loading (minimum tension field).

(a) Column Elevation View **(b) Close-up View of a Typical Crack**

Figure 2-1. Cracking in Column under Axial Compression Loads (Houston, TX).

(a) Elevation View and Typical Cracking on Tension Face (Houston, TX).

(b) Elevation View (San Antonio, TX)

Figure 2-2. Cracking in Cantilevered Bents under Axial and Overturning Moments.

Figure 2-3. Cracking in Bent Cap under Minimal External Loading (Houston, TX).

CHAPTER 3: SUMMARY OF THE EXPERIMENTAL PROGRAM

In order to assess the structural behavior of bridge column splices that are influenced by ASR/DEF, a comprehensive experimental program was conducted over an 8-year period. The following sections summarize the details and findings of the program.

3.1 SPECIMEN DESIGN AND CONSTRUCTION

This research focused on the performance of the splice region of a typical reinforced concrete bridge column in Texas primarily under axial compression loading and subject to ASR and/or DEF. Because in-service bridge columns can vary considerably in size and geometry, a large-scale column (LSC) specimen was designed to utilize a common splice found in the field at the column/foundation connection, which is typical in non-seismic regions. Because the strength of the lap splice depends on the bond, the effects of both ASR and/or DEF expansion on the bond are causes for concern. If the bond is decreased enough that the bars slip prior to reaching their yield strength, the capacity of the column may not be high enough to resist the ultimate structural demands and failure might be possible.

In an effort to reduce costs and maximize the specimen size based on the constraints of the testing laboratory, the research team used 16 LSC specimens in the experimental research program. Specimens were 2 ft × 4 ft (0.61 m x 1.22 m) in cross section with six #11 bars overlapped in the 9 ft (2.74 m) splice region, which is the same overlap length TxDOT used in the field structures examined.

Figure 3-1 and Figure 3-2 show the dimensions and rebar layout of the LSC specimens.

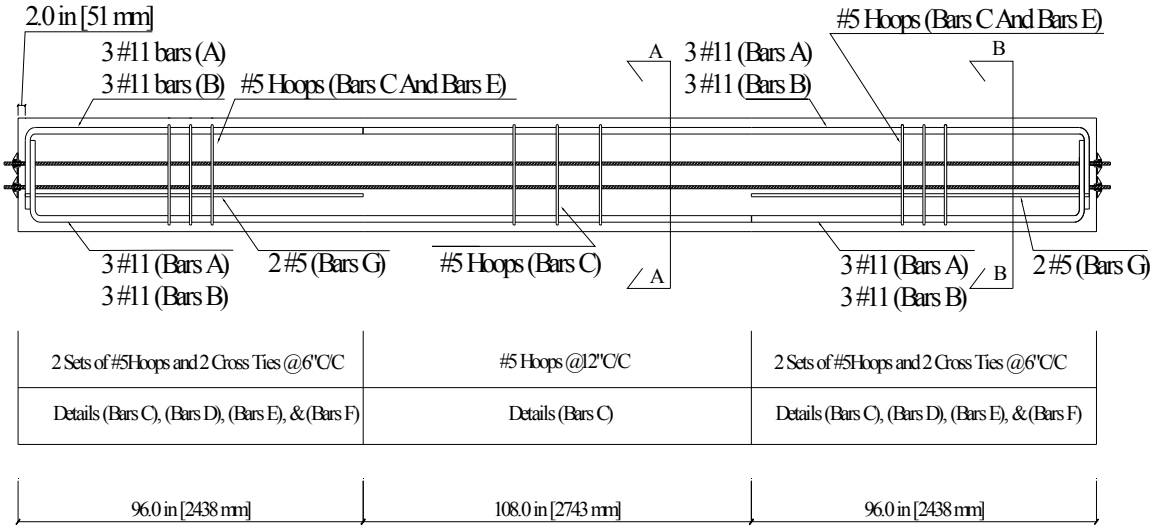

Figure 3-1. Reinforcement Layout.

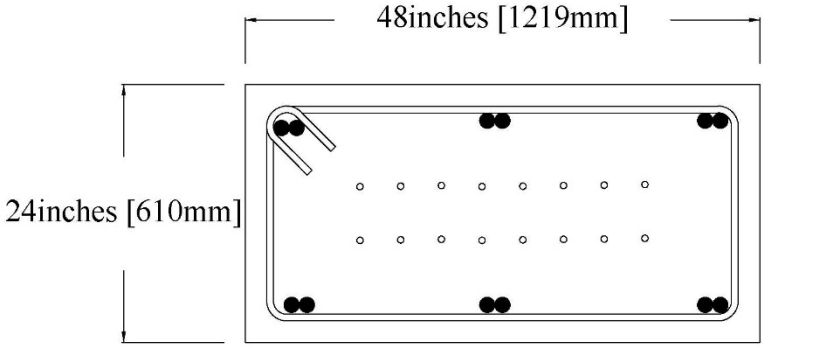

Section A-A Splice Region

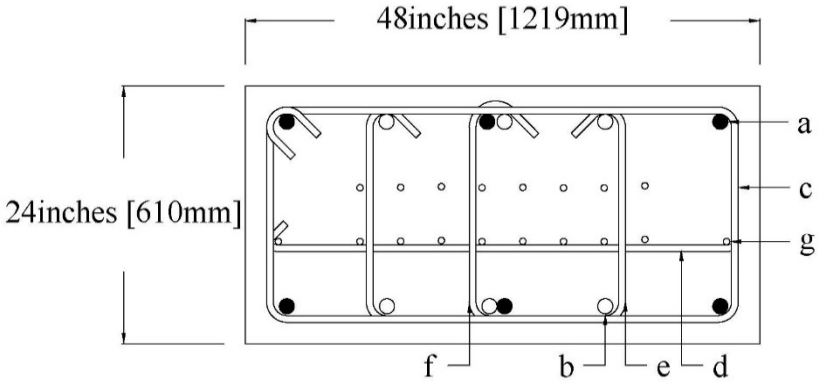

Section B-B End Region

Section B-B Parts	
a	6 #11 Bars A [marked with fill]
b	6 #11 Bars B [marked without fill]
c	#5 Hoops @ 6" C/C (Bars C)
d	#5 Cross Ties @ 6" C/C (Bars D)
e	#5 Hoops @ 6" C/C (Bars E)
f	#5 Cross Ties @ 6" C/C (Bars F)
g	2 #5 Bars (Bars G)

Figure 3-2. Cross Section View of the Reinforcement Layout.

In publications by the American Concrete Institute (ACI 318, 2008) and American Association of State and Highway Transportation Officials (AASHTO, 2004), the required splice length is a function of the required development length of the bar (l_d) and various factors. According to ACI 318 (2008), for #11 bars with f'_c = 5000 psi (34.5 MPa), the required development length is 46.7 inches (1.19 m). Therefore, the provided splice length of 9 ft (2.74 m) in the LSC specimens corresponds to 2.3 x l_d. A Class B splice length (when the area of reinforcement provided is not at least twice what the analysis required over the entire length of the splice and when the splice is staggered) is required to have 1.3 x l_d, which means that the provided splice length is overdesigned by 78 percent. According to AASHTO (2004), the required development length for a #11 bar is 52 inches (1.32 m). Therefore, the provided splice length in the LSC

specimens corresponds to 2.08 x l_d. In AASHTO (2004), this splice is required to have a Class C splice, which requires the splice length to be 1.7 x l_d, implying that the splice is overdesigned by 22 percent. Both ACI 318 (2008) and AASHTO (2004) show this splice to be conservatively designed. The question is whether the effects of ASR and/or DEF will deteriorate the bond of the column reinforcing steel in the splice region enough to overcome the conservative design.

To simulate in-service gravity loading on the bridge column, the specimens had sixteen 0.6 inch (15 mm) diameter, unbonded, post-tensioning (PT) strands. The PT strands were centered throughout the specimen cross section (see Figure 3-2). The strands were hydraulically jacked to 0.7 f_{pu}, ultimate tensile stress, according to AASHTO (2007), which resulted in 36.3 kips (161.47 kN) per strand and a total of 580.5 kips (2582.19 kN) of compression on the column specimen. This level of axial load corresponded to about 10 percent of the axial compression strength of the column, which is commonly found in columns under service loading.

3.2 CONCRETE MATERIALS TO PROMOTE ASR/DEF

Due to the limited time of the research program, the materials of construction and the curing conditions for the specimens were carefully designed to aggressively promote and accelerate ASR. The coarse and fine aggregates were selected based on reactivity to promote ASR in the concrete. Type III cement from Lehigh Cement in Evansville, Pennsylvania, was used because of the high alkali content to promote ASR in the LSC specimens. To further increase the alkalis in the concrete mixture, sodium hydroxide (NaOH) was added to the mix. The cement contributed 6.62 lb/cy (3.93 kg/m^3) of alkalis, and the added sodium hydroxide contributed an additional 3.28 lb/cy (1.95 kg/m^3), resulting in a total alkali content of 9.9 lb/cy (5.87 kg/m^3).

Table 3-1 shows the mixture characteristics and Table 3-2 shows the mixture proportions used for the LSC specimens. The target compressive strength of the concrete mixture was 5,000 psi (34.5 MPa).

Table 3-1. Mixture Characteristics.

Material	Mix Values
Coarse Aggregate (absorption capacity in %)	0.96
Fine Aggregate (absorption capacity in %)	0.65
NaOH	51.3 lb in 21.14 gal (23.3 kg in 80 L)
Anticipated Air Content (%)	1.0
Specific Gravity of the Cement	3.15
Specific Gravity of the Coarse Aggregates	2.57
Specific Gravity of the Fine Aggregates	2.65

Table 3-2. Mixture Proportions.

Material	SSD (lb/yd^3)
Cement	752
Course Aggregate	1350
Fine Aggregate	1438
Water	361
NaOH	5.7
Water/Cement	0.48

3.3 REINFORCING STEEL

The research team used Grade 60 reinforcing steel meeting American Society for Testing and Materials (ASTM) A615 specifications to fabricate the LSC specimens. From tension coupon testing, the yield strength of the reinforcement was about 65 ksi, and significant deformability beyond yielding was achieved.

3.4 CURING CONDITIONS

To promote DEF, the LSC specimens were supplemented with heat by electrical resistive wiring (ERW) to ensure that the concrete temperature throughout the critical splice region was above 160°F (71.1°C) during the curing of the concrete. Researchers preinstalled the ERW in the bottom and top forms and then covered with stainless steel and insulation. In addition, ERW was required in the mid-depth of the LSC specimens by one-dimensional heat-flow analysis. The ERW was pushed through cross-linked polyethylene tubing that was strung through the vertical center of the cross section of the LSC specimens at four points and passed through the end of the form. The ERW solution consisted of three controllable sections to apply heat, which allowed for a more uniform temperature distribution in the concrete throughout the specimen. Shortly after the concrete was poured into the formwork, the ERW control system was activated such that the concrete temperatures at varying depths would be at least 160°F (71°C) for about 48 hours. Figure 3-3 shows sample thermocouple readings in the concrete during curing and shows that temperatures exceeded 180°F (82°C), therefore promoting the conditions for DEF. After about 48 hours, the ERW control system was turned off and the specimen was allowed to gradually cool to reduce thermal cracking.

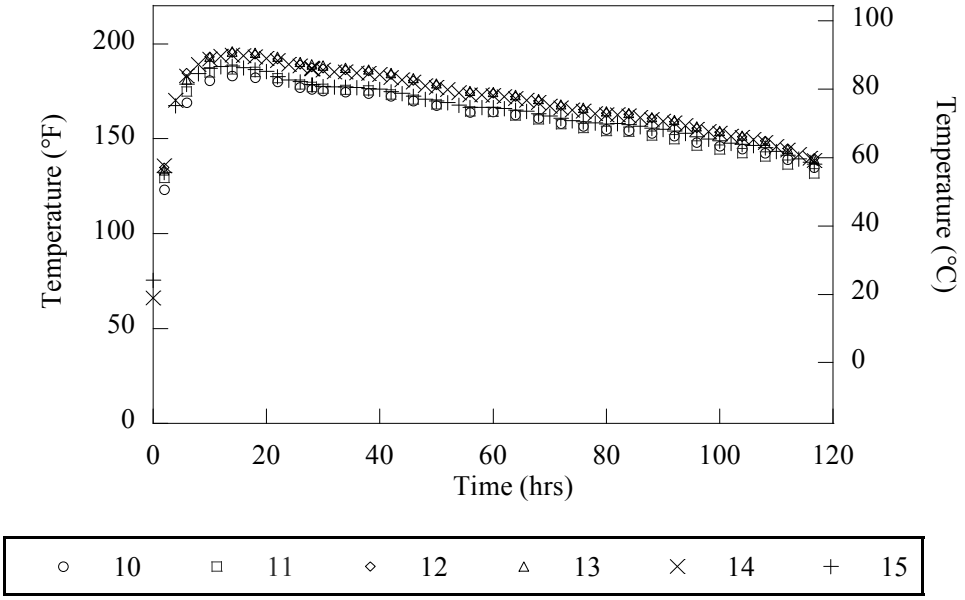

Horizontal Measurements

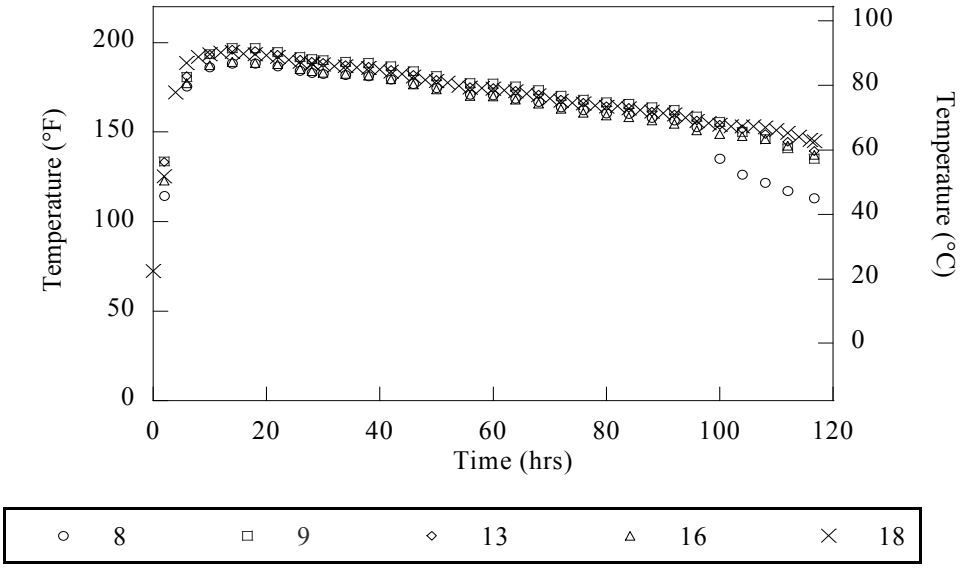

Vertical Measurements

Figure 3-3. Typical Temperature History at Mid-Span Cross Section.

3.5 AGGRESSIVE EXPOSURE PROGRAM

Shortly after the construction of LSC specimens and application of the preload to simulate gravity loading from in-service conditions, the specimens were placed outside at the Texas A&M University Riverside Campus in Bryan, Texas, where they were exposed to the environmental weather conditions of the area and supplemental water to accelerate the ASR and DEF

deterioration mechanisms (see Figures 3-4 and 3-5). A sprinkler system activated four times a day and for 15 minutes each time supplied the supplemental water.

Figure 3-4. LSC Specimens Exposed to the Environment at the Riverside Campus.

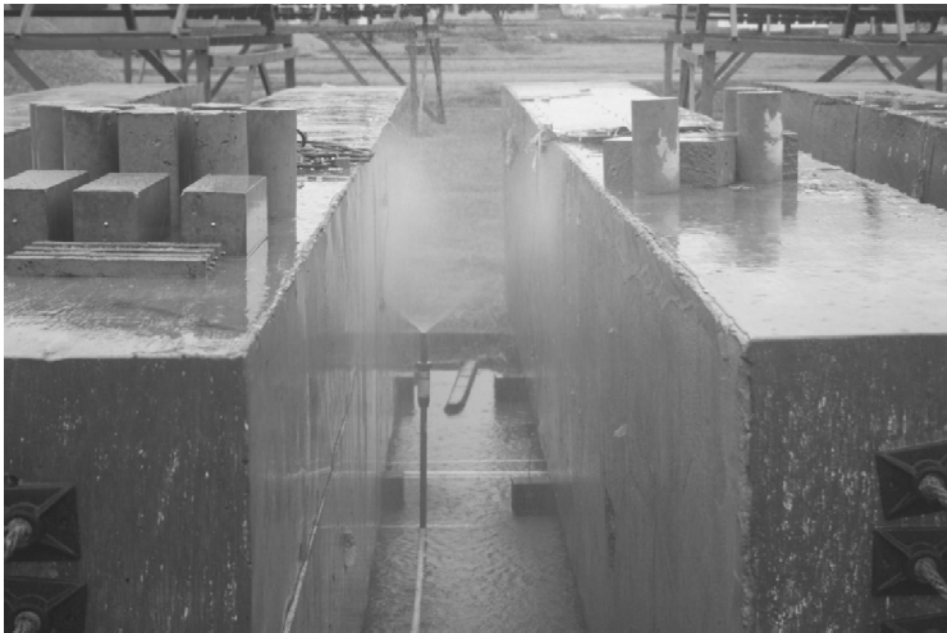

Figure 3-5. Sprinkler System between Two LSC Specimens.

The LSC specimens were rotated twice during the exposure program to provide more uniform expansion throughout the specimens. Since the small face (SF) at the bottom had not experienced any direct sunlight in the first orientation, during the first rotation, researchers positioned it on top. The second rotation was 90 degrees about the longitudinal axis of the member, which

positioned the large face (LF) of the column on top. This large face was the critical tension splice region during structural testing, as explained in the next section.

The behavior of the LSC specimens during the environmental exposure conditions was monitored with external and internal measuring devices. Demountable mechanical (DEMEC) points were mounted on the surface of the specimens and provided a way to measure the external surface deformations using a caliper during the exposure phase (see Figure 3-6). Electronic strain gages were placed on the reinforcing steel, and concrete embedment gages were placed within the concrete specimen to measure the internal deformations during the exposure phase. Tables 3-3 and 3-4 summarize specimen age at structural testing, measured surface expansions and concrete crack widths on the different faces of the specimens, and estimated degrees of ASR and DEF at the time of structural testing, which were determined based on the surface strains and cracking, measured internal strains, and petrography analysis of concrete cores taken from the specimens after they were structurally tested.

Figure 3-6. DEMEC Surface Strain Measurements.

Table 3-3. Specimen Age and Degree of Deterioration.

LSC Specimen #	Date of Casting	Date of Initial Exposure	Date of Structural Load Test	Degree ASR	Degree DEF
1	1/2008	5/2008	8/2010	M/L	N/E
3	2/2008	5/2008	8/2010	M/L	N/E
4	3/2008	5/2008	6/2014	*	*
5	4/2008	5/2008	7/2011	M/L	N/E
8	5/2008	7/2008	7/2011	M/L	N/E
9	6/2008	7/2008	2/2010	M/L	N/E
10	6/2008	7/2008	2/2010	M/L	N/E
12	7/2008	9/2008	6/2014	*	*
15	8/2008	N/A	2/2009	N	N
16	8/2008	N/A	2/2009	N	N

NOTE: N/A = specimen was not exposed to environmental exposure conditions; N = none; E = early stage; M = middle stage; L = late stage. These stages were established based on the petrography analysis of concrete cores taken from specimens after structural testing and from the surface and internal expansion measurements and cracking throughout the specimen prior to testing.

* Results of the petrography analysis were not available at the time of the publication of this report. However, the expansion and amount of cracking were more than in other specimens previously tested. In addition, the rate of expansion and amount of cracking had leveled over the prior three years, as compared to the first three years of exposure.

Table 3-4. Specimen Surface Expansions.

LSC #	Average Transverse Surface Strain at Time of Load Test (strain)				Maximum Crack Width at Time of Load Test (inch [mm])			
	Small Face 1	Small Face 2	Large Face 1	Large Face 2	Small Face 1	Small Face 2	Large Face 1	Large Face 2
1	0.0064	0.0024	0.0070	NT	0.03 (0.8)	0.04 (1.0)	0.04 (1.0)	NT
3	0.0067	0.0026	0.0054	NT	0.04 (0.9)	0.03 (0.6)	0.03 (0.6)	NT
4	*	*	*	0.0172	0.06 (1.3)	0.06 (1.3)	0.12 (2.5)	0.06 (1.3)
5	0.0080	0.0087	0.0090	0.0123	0.03 (0.6)	0.03 (0.6)	0.03 (0.6)	0.04 (1.0)
8	0.0082	0.0092	0.0088	0.0112	0.01 (0.3)	0.03 (0.8)	0.03 (0.8)	0.03 (0.6)
9	0.0051	0.0009	0.0026	NT	0.01 (0.2)	0.01 (0.2)	0.01 (0.2)	NT
10	0.0052	0.0013	0.0038	NT	0.01 (0.2)	0.02 (0.4)	0.02 (0.4)	NT
12	*	*	*	0.0125	0.06 (1.3)	0.06 (1.3)	0.06 (1.3)	0.05 (1.2)
15	N/A	N/A	N/A	N/A	N/A	N/A	N/A	N/A
16	N/A	N/A	N/A	N/A	N/A	N/A	N/A	N/A

NOTE: N/A = data not taken but presumed to be minimal; NT = data not taken but presumed similar to that on Large Face 1.
* Data not taken during project extension phase.

Figures 3-7, 3-8, and 3-9 show sample cracking that developed throughout the exposure phase for LSC Specimens #1, #8, and #12, with about 2.3, 3.0, and 5.8 years of exposure, respectively. The figures show that substantial cracking resulted and the cracking pattern was similar between the specimens, even though the exposure periods of the specimens varied. LSC Specimens #1 and #8 had similar crack widths; however, Specimen #12 had some much larger crack widths (about two times those of Specimens #1 and #8, as reported in Table 3-4). The specimen cracking, as shown in Figures 3-7, 3-8, and 3-9, is comparable to the cracking in actual field structures affected by ASR (see Figure 2-1).

Figure 3-7. Cracking of Specimen #1 prior to Structural Load Testing.

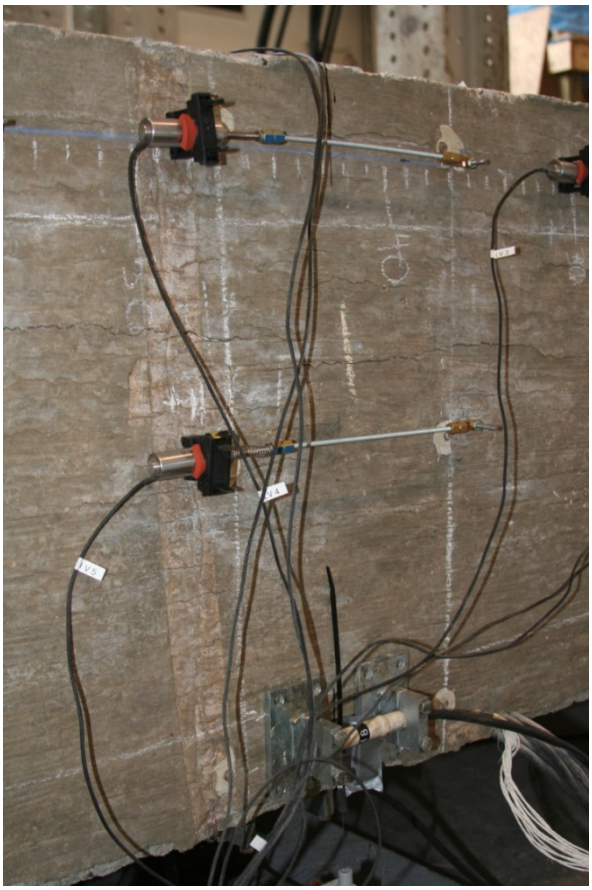

Figure 3-8. Cracking of Specimen #8 prior to Structural Load Testing.

Figure 3-9. Cracking of Specimen #12 prior to Structural Load Testing.

In existing bridge columns, crack widths can be measured quite easily using crack width comparator cards or crack width measuring devices, while other strain data are more difficult to obtain since instrumentation may not be installed prior to construction. However, the surface strains calculated with the DEMECs in this research more accurately represent the total surface expansion since small cracks are difficult to measure and concrete expansion between the cracks due to ASR/DEF was not considered. Therefore, the strains from crack width measurements in the large-scale specimens (determined by summing the measured crack widths in a given region between fixed DEMEC points divided by the distance between those points) were compared to the strains computed using the caliper readings of the DEMEC points. Bracci et al. (2012) and Bracci (2014) showed that transverse expansion strains determined by summing the crack widths generally were about 50 percent of the average surface strain using the caliper DEMEC point measurements. This reduced strain from the sum of the crack widths can be explained by the expansion of the concrete between cracks that was not accounted for and other cracks that were too small to measure.

In summary, 14 large-scale specimens stored at the Riverside Campus were exposed to outdoor weather conditions in Bryan, Texas, and to wet-dry cycles using supplemental water to accelerate the ASR/DEF deterioration mechanisms. The research team continually recorded internal instrumentation and external surface measurements for all specimens throughout the exposure phase. From these measurements and surface cracking inspections, it can be concluded that all specimens successfully developed significant concrete expansive strains and surface cracking due to varying levels of primarily ASR and minimal DEF. The observed cracking

pattern is also representative of observations of in-service bridges believed to be affected by ASR. In addition, the deterioration mechanism is continuing, but at a much slower rate over that past three years as compared to the first three years of exposure. It is believed that additional exposure time may lead to more significant DEF development, which can potentially be more damaging due to larger reported expansions in the literature. Therefore, beyond the TxDOT-funded phase of the research, six of the untested specimens will remain at the Riverside Campus permanently exposed only to the outdoor environmental conditions of the area (the sprinkler system was removed), and researchers will periodically inspect the specimens.

The following list highlights some of the findings derived from the exposure program to date, based on Bracci et al. (2012) and Bracci (2014):

- Direct sunlight and wet-dry cycles on the specimens had a significant impact on the expansion due to ASR. The transverse concrete surface expansion of the side face, LF1, of the specimen, closest to the top surface, only reached 61 percent of the transverse expansion on the top surface (SF1), and an average of the other three transverse strains on the side face closer to the ground (SF2) reached only 22 percent of the expansion on the top surface (SF1) before the specimens were first rotated.
- The LSC specimens expanded at higher strain rates during the first summer months as compared to non-summer months. The expansion in the summer months varied from 1.7 to 6.5 times the non-summer months for the three groups of specimens depending on when they were first exposed to summer temperatures since specimens were placed at the exposure site at varying times of the year.
- The transverse surface strains were about 10 times larger than the longitudinal surface strains due to the longitudinal restraint from the axial post-tensioning steel and longitudinal column reinforcement.
- The average strains calculated from measuring the sum of the crack widths between DEMEC points using crack card indicators converged over time to about 50 percent of the surface strains calculated from measuring the distance between DEMEC points by a caliper. This means that about half of the surface strain was due to the strain in the concrete between cracks and due to smaller cracks that were not measured.
- The measured strains were larger on the surface than on the inside of the specimen. The strain in the cover was about 58 percent of the surface strain, and the strain in the core concrete was about 52 percent of the surface strain. The strain in the transverse reinforcement in the middle of the splice region had different values on the small and large faces. These strains were 0.0036 and 0.0054 on SF1 and LF1, respectively, which exceeded the yield strain of the reinforcement. The transverse hoop strains, as a percentage of the concrete surface strain, were 40 percent on SF1 at the time of the first rotation and were 83 percent and 78 percent on LF1 at the first two rotations, respectively.
- Using measured internal and external concrete expansion data, measured crack widths, and results from petrography analyses of concrete cores taken from the specimens after they were structurally tested, researchers categorized the tested specimens as having no to later-stages ASR and either no occurring or minimal DEF. However, the petrography analysis for the last two specimens (LSC4 and LSC12) tested during the project extension phase was not available at the time of this report.

3.6 EXPERIMENTAL TEST SETUP

To evaluate the experimental performance of the splice regions, the LSC specimens were first load tested to near failure using a four-point load test. Figure 3-10 shows that in a four-point load test, a constant moment is applied over the splice region, which allows for the weakest section of the region to crack, yield, and ultimately fail. In this test setup, a constant tension force across the entire splice length is created in the bottom longitudinal reinforcement. For an in-service cantilevered bridge column under lateral loading, the bending moment in the column varies linearly from zero at the top to maximum at the column base, which implies that the splice reinforcement is not loaded uniformly along its length. However, the test setup will yield conservative values in terms of the splice performance.

Following the four-point load test, researchers tested the LSC specimens using a three-point test setup, except for LSC Specimens #4 and #12. Figure 3-11 shows that a three-point test creates a uniform shear force throughout the splice region and a linearly increasing moment demand from zero at the loading points to maximum at the reaction support. Since the peak moment demand for the splice (largest tensile stresses) is at the very center of the splice region and the entire splice region has load-induced shear demands, the overall demands on the splice length region might be somewhat more critical than in the previous test, although not realistic in terms of loadings on in-service structures.

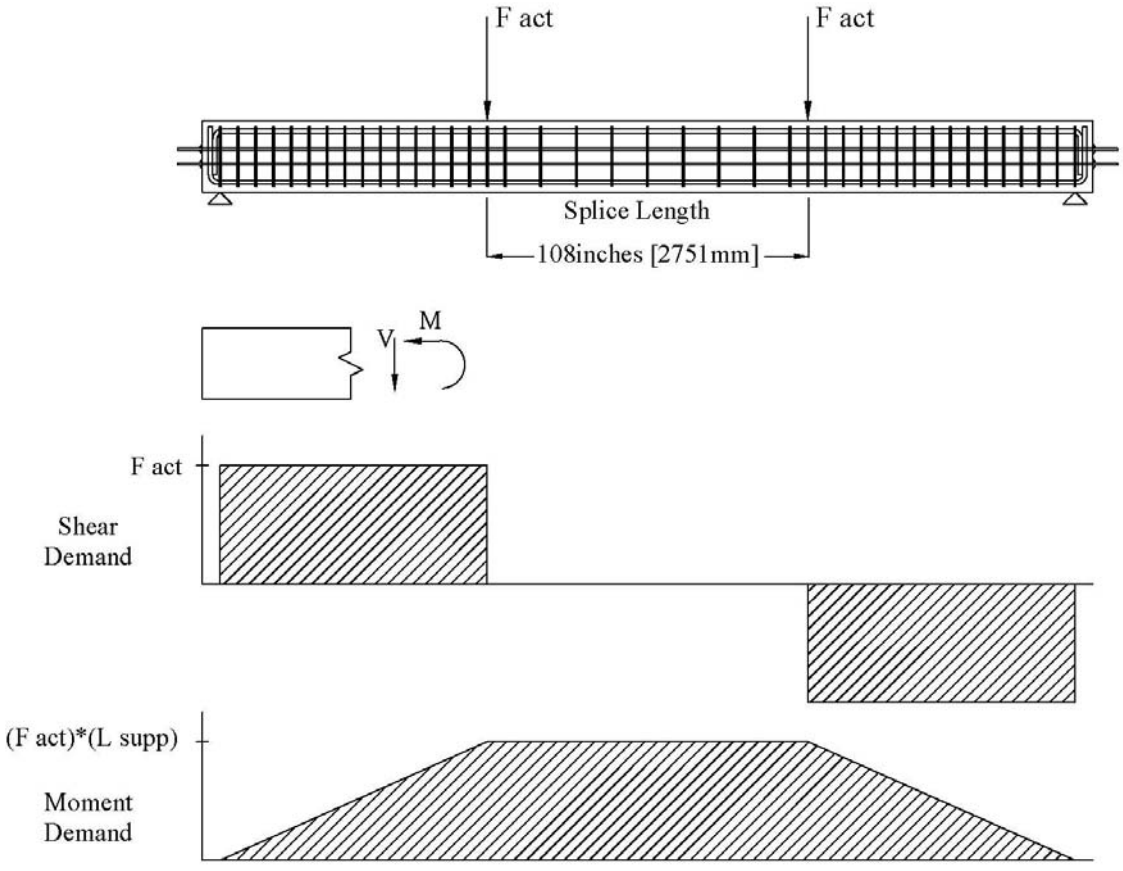

Figure 3-10. Four-Point Load Test.

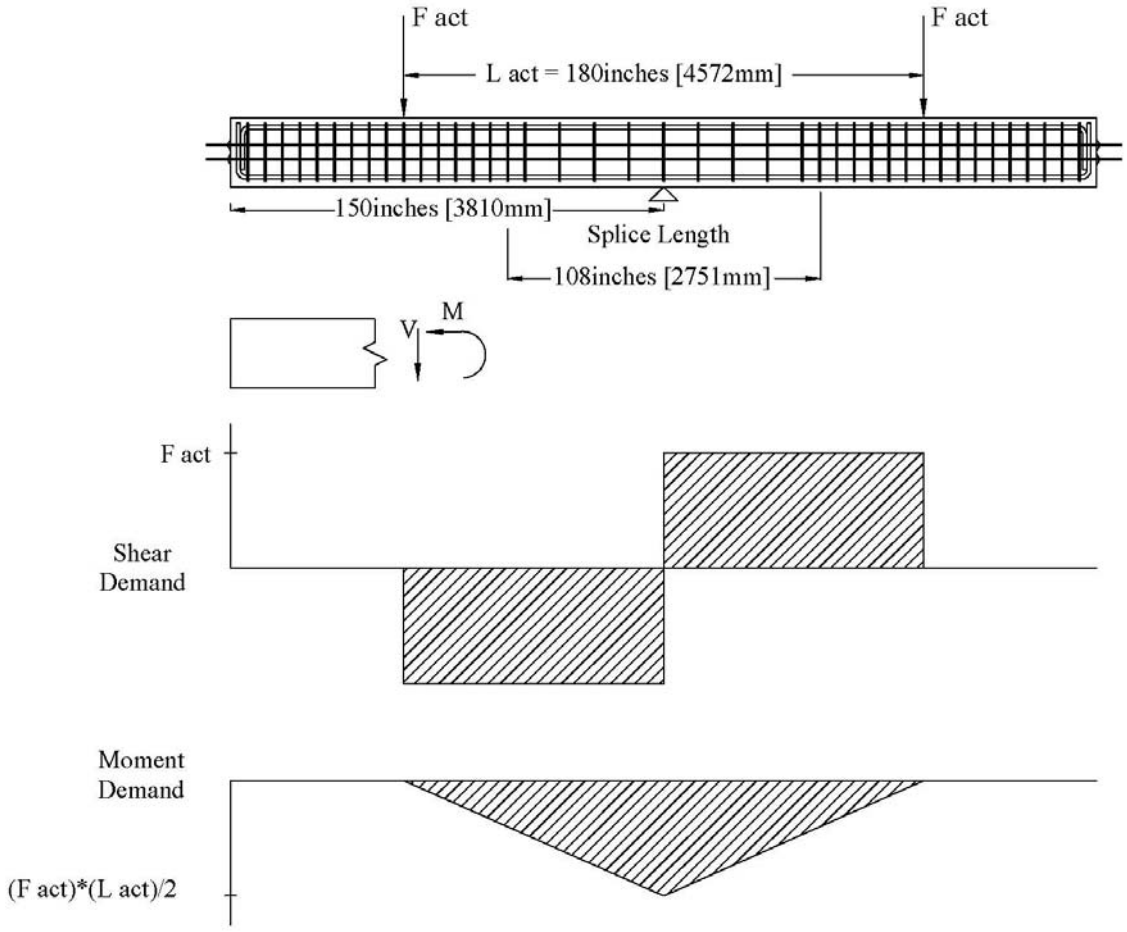

Figure 3-11. Three-Point Load Test.

3.7 STRUCTURAL PERFORMANCE DURING VARYING STAGES OF MOSTLY ASR

Figure 3-12 shows the measured force-deformation behavior of the control specimens (LSC15 and LSC16) and those with varying degrees of primarily ASR (and minimal DEF), as identified in Tables 3-3 and 3-4, during the four-point test setup prior to the project extension phase (originally reported by Bracci et al. 2012). Figures 3-13 and 3-14 show the measured force-deformation behavior of LSC Specimens #12 and #4 tested during the project extension phase with increasing levels of concrete expansion and cracking due to primarily ASR (and minimal DEF), as identified in Tables 3-3 and 3-4, during the four-point test setup. The figures show that the structural behaviors of Specimens #12 and #4 are comparable to those specimens tested early in the research project that were influenced by ASR. In particular, the structural testing of Specimen #4 was taken to significantly larger deformations (terminated close to when the researchers deemed structural failure was eminent) in order to get an indication of structural ductility capability of the spliced region. Also, the structural response of the specimen at around 1 inch displacement seemed to have unloaded at one actuator point and further loaded at the other actuator point. This response developed due to a slight shift in the physical supports at the

specimen end because of the elongation of the specimen at the bottom. Once the supports stabilized, actuator loadings continued as expected for the test setup under displacement control loading.

As seen by comparing Figures 3-12, 3-13, and 3-14, the specimens with varying degrees of ASR showed no evidence of bond deterioration within the splice, had similar initial stiffness and behavior up to the first cracking, had a 25 to 35 percent increase in post-cracking stiffness up to yielding, had a 5 to 15 percent increase in yield strength, and showed no overall detrimental effects on the structural response when compared to control specimens without ASR deterioration. This improved behavior can be explained by the resulting volumetric expansion of the concrete due to ASR that engaged the longitudinal and transverse reinforcement, which is believed to have resulted in increased axial loading and better confinement of the core concrete.

Based on Bracci et al. (2012), Figure 3-15 shows the measured force-deformation behavior of the control specimens (LSC15 and LSC16) and those with varying degrees of primarily ASR (and minimal DEF), as identified in Tables 3-3 and 3-4, during the three-point test setup prior to the project extension phase. Note that the three-point loading test setup was not performed on Specimens #12 and #4. Figure 3-15 also shows improved structural behavior in specimens affected by ASR compared to the control specimens.

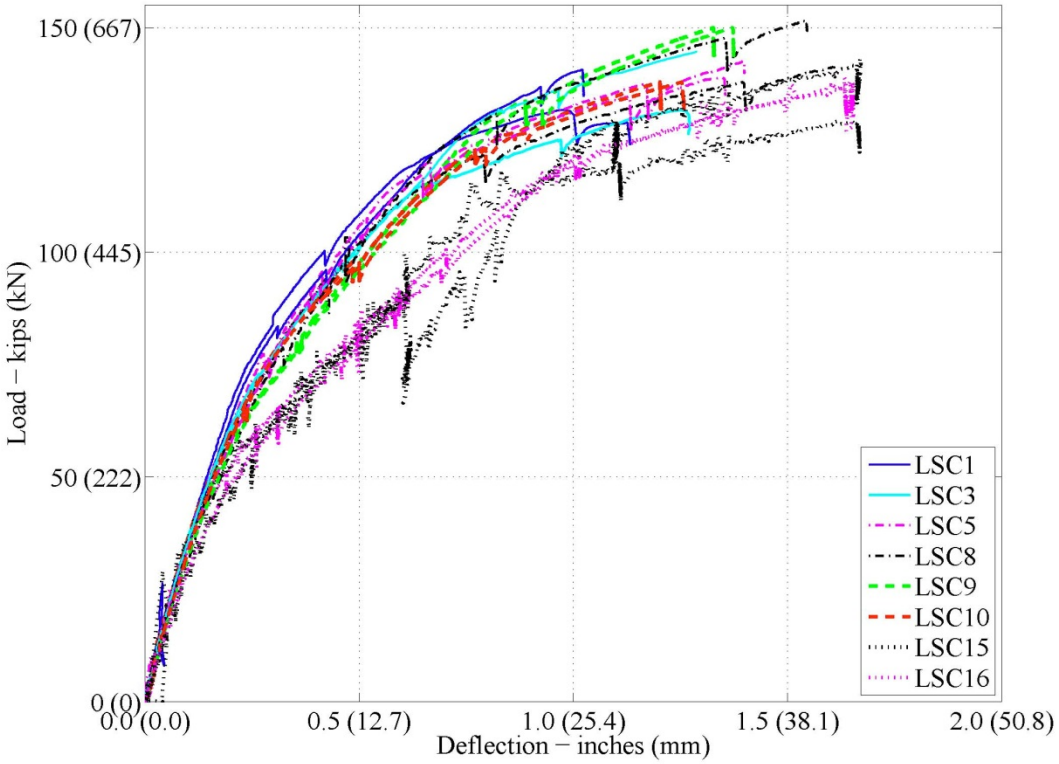

Figure 3-12. Experimental Load vs. Deflection during Four-Point Test: Specimen Behavior at the Actuator Load Point (Splice End) (Bracci et al. 2012)

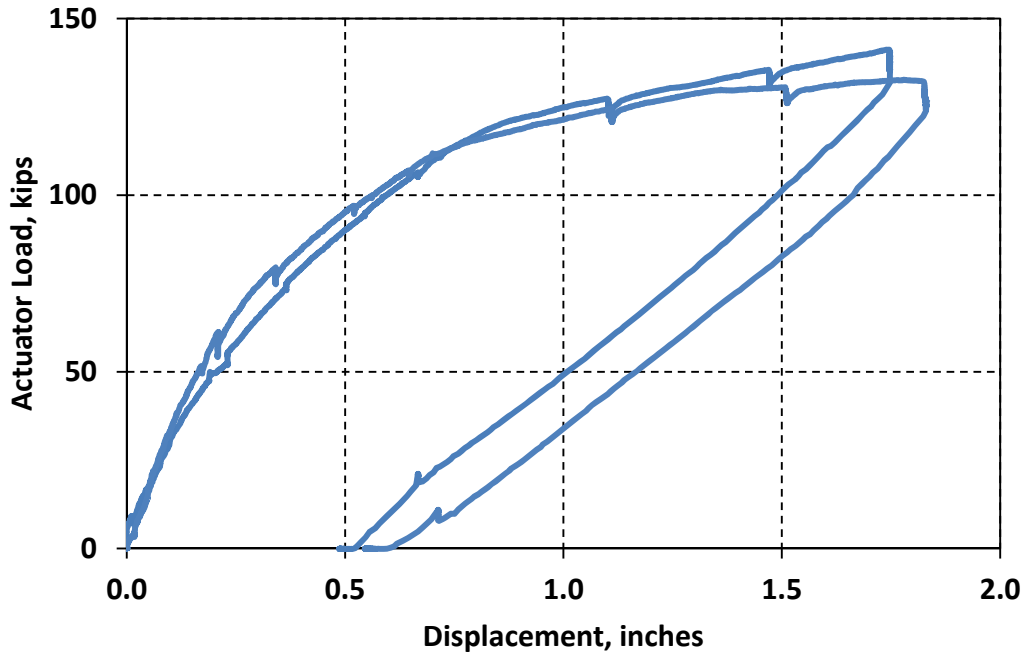

Figure 3-13. Experimental Load vs. Deflection during Four-Point Test: Specimen LSC12 Behavior at the Actuator Load Point (Splice End).

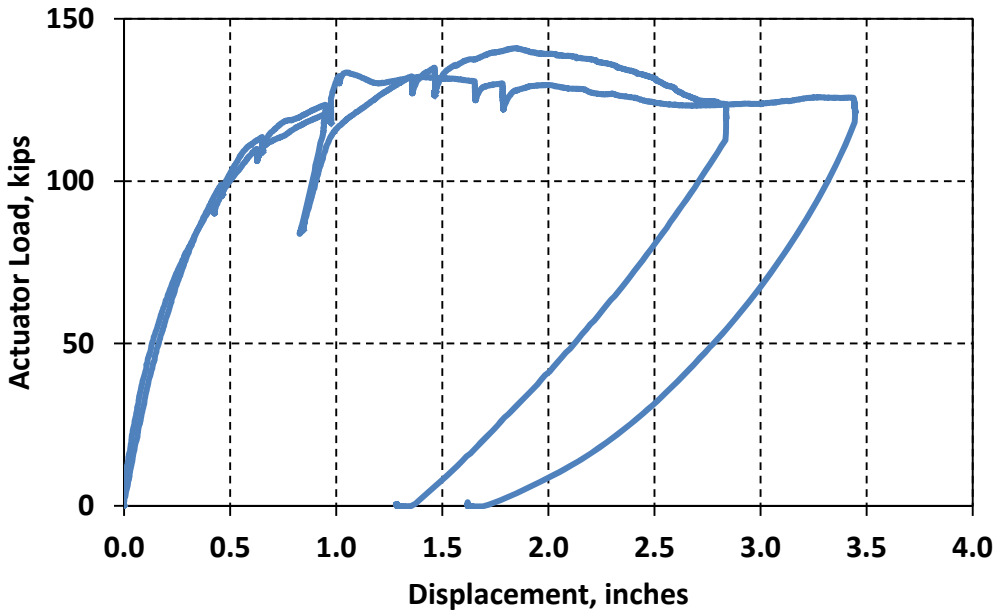

Figure 3-14. Experimental Load vs. Deflection during Four-Point Test: Specimen LSC4 Behavior at the Actuator Load Point (Splice End).

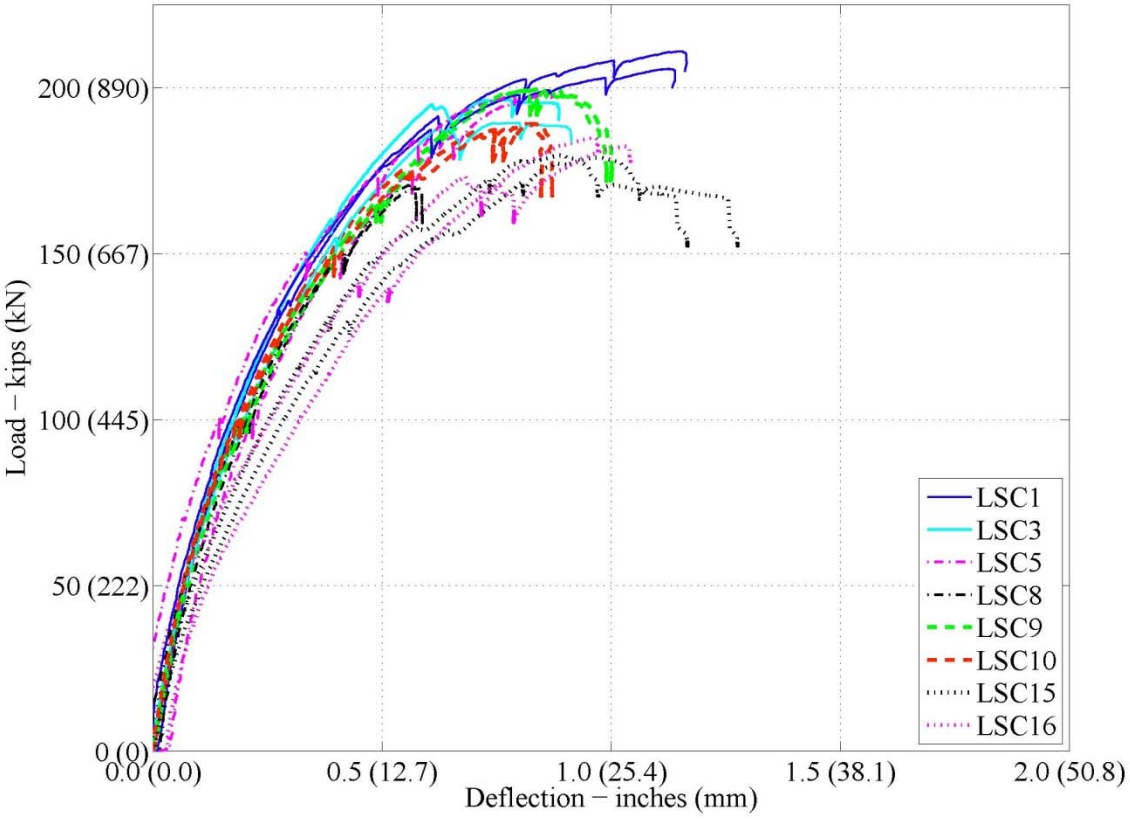

Figure 3-15. Experimental Load vs. Deflection during Three-Point Test: Specimen Behavior at the Actuator Load Point (Bracci et al. 2012)

3.8 CONCLUSIONS

The experimental program consisted of the design, construction, curing, exposure, testing, and assessment of 16 large-scale column specimens (under concentric axial loading due to service conditions) with a lap splice region typical of TxDOT practice for the bar size being used and conservative by code standards. This report presents a summary of the results on the testing of 10 of these specimens. Two control specimens exhibited no ASR/DEF deterioration, and four groups of two specimens exhibited varying levels of ASR deterioration up to middle to late stages and minimal DEF in terms of presence and degree of expansion (note that the results of the petrography analysis of the last two specimens tested were not available at the time of this reporting). All 10 specimens were structurally load tested in the four-point load test setup, and all but the last two specimens were tested in the three-point load test setup. Six additional specimens are being stored at the exposure site indefinitely under outdoor exposure conditions and will periodically be inspected by the researchers on an unfunded basis.

The key findings from the test program are the following:

- The structural behavior of specimens with varying degrees of ASR up to middle to late stages showed no discernible evidence of bond deterioration of the splice region.
- In comparison with the response of the control specimens, specimens exhibiting ASR had similar initial stiffness and behavior up to first cracking, had about a 25 to 35 percent increase in post-cracking stiffness up to yielding, had about a 5 to 15 percent increase in yield strength, and showed no overall detrimental effects on the structural response. The increase in stiffness and strength can be explained by the resulting volumetric expansion of the concrete due to the ASR that engaged the transverse reinforcement for better confinement of the core concrete and engaged the supplemental post-tensioning reinforcement and the column longitudinal reinforcement to generate additional axial compression load.
- The vulnerability of the column splice with increased levels of DEF deterioration could not be evaluated to date. In spite of the research team's best efforts to accelerate deterioration resulting from DEF, more time and possibly different exposure conditions are needed to allow the remaining six specimens to further deteriorate.

3.9 RECOMMENDATIONS

Although results from the experimental program indicate that middle- to late-stage ASR did not significantly influence the performance of the specimen lap splice regions with concentric axial loading due to service conditions, care should be taken when applying these results and findings to other structural applications. The lap splice length in the specimens tested was overdesigned per TxDOT standards for the bar size being used, and less conservative designs may exhibit different behavior. The splice region in the specimens tested also had a single full column hoop at typical 12 inch spacing that provided sufficient confinement of the concrete core region. In members without proper confining steel or proper longitudinal steel, special monitoring of developing crack patterns and crack widths should take place in assessing the structural capability since this task was beyond the scope of the research performed. In addition, because the ASR process was accelerated and testing was performed at relatively early ages in the research, longer-term deterioration may result in different specimen performance.

At the date of this report, it appears that most of the expansion and cracking in the specimens primarily occurred due to ASR and minimal DEF. DEF and other deterioration mechanisms, such as corrosion, may develop over time since significant cracking due to ASR will allow for more water and corrosive substances to penetrate into the concrete cover and core regions. These deterioration mechanisms were not addressed in this report and will need to be fully studied experimentally for their effects on the structural performance of column splice regions.

In structures suspected to be influenced by ASR and other deterioration mechanisms, careful monitoring of developing crack patterns and crack widths should be recorded and carefully studied. When crack widths exceed those typical for in-service structures and when cracking patterns become identifiable, petrography analysis of concrete cores taken from the structure should be performed to identify the developing expansion mechanism in the concrete. In addition, the provided reinforcing steel should be carefully identified and assessed for strength and for transverse confinement of the concrete core region when the concrete may be exposed to expansive pressures.

In addition, this report documents the developing maximum crack width measurements and the surface strain measurements—via precious caliper readings and by summing of cracks measured with a crack width card indicator in a given region—that developed in this experimental program on large-scale column specimens. When measured crack widths and surface strains in actual bridge structures exceed the values of those in this report, special care should be exercised to assess the structural capability of the splice regions since this task was beyond the scope of the research performed.

REFERENCES

ACI 318. "Building Code Requirements for Structural Concrete (ACI 318-08) and Commentary," American Concrete Institute, Farmington Hills, MI, 2008.

AASHTO. "LRFD Bridge Design Specifications," American Association of State Highway and Transportation Officials, Washington, D.C., 2004.

AASHTO. "LRFD Bridge Design Specifications," American Association of State Highway and Transportation Officials, Washington, D.C., 2007.

Bae, S., O. Bayrak, J.O. Jirsa, and R.E. Klingner. "Anchor Bolt Behavior in ASR/DEF-Damaged Drilled Shafts," Technical Report IAC 88-5DDIA004, The University of Texas at Austin, TX, 2007.

Bauer, S., B. Cornell, D. Figurski, T. Ley, J. Miralles, and K. Folliard. "Alkali-Silica Reaction and Delayed Ettringite Formation in Concrete: A Literature Review," Report No. FHWA/TX-06/0-4085-1, Center for Transportation Research, The University of Texas at Austin, TX, 2006.

Berube, M.-A., D. Chouinard, M. Pigeon, J. Frenette, L. Boisvert, and M. Rivest. "Effectiveness of Sealers in Counteracting Alkali-Silica Reaction in Plain and Air-Entrained Laboratory Concrete Exposed to Wetting and Drying, Freezing and Thawing, and Salt Water," *Canadian Journal of Civil Engineering*, 29, 2002, 289–300.

Bracci, J.M. "Performance of Lap Splices in Large-Scale Column Specimens Affected by ASR and/or DEF—Extension Phase," Report 0-5722-2, Texas Transportation Institute, Texas A&M University, 2014, under current development.

Bracci, J.M., P. Gardoni, M. Kathleen Eck, and D. Trejo. "Performance of Lap Splices in Large-Scale Column Specimens Affected by ASR and/or DEF," Report 0-5722-1, Texas Transportation Institute, Texas A&M University, 2012.

Burgher, B., A. Thibonnier, K.J. Folliard, T. Ley, and M. Thomas. "Investigation of the Internal Stresses Caused by Delayed Ettringite Formation in Concrete," Technical Report No. FHWA/TX-09/0-5218-1, Center for Transportation Research, The University of Texas at Austin, 2008.

Canadian Standards Association. "Guide to the Evaluation and Management of Concrete Structures Affected by Alkali-Aggregate Reaction," Canadian Standards Association, CSA A864-00, Mississauga, ON, Canada, 2000, 108p.

Eck Olave, M.K., J.M. Bracci, P. Gardoni, and D. Trejo. "Performance of RC Columns Affected by ASR: Accelerated Exposure and Damage," *ASCE Journal of Bridge Engineering*, 2014a, in print.

Eck Olave, M.K., J.M. Bracci, P. Gardoni, and D. Trejo. "Performance of RC Columns Affected by ASR: Experiments and Assessment," *ASCE Journal of Bridge Engineering*, 2014b, in print.

Fan, S., and J.M. Hanson. "Effect of Alkali Silica Reaction Expansion and Cracking on Structural Behavior of Reinforced Concrete Beams," *ACI Structural Journal*, Vol. 95, No. 5, 1998a, 498–505.

Fan, S., and J.M. Hanson. "Length Expansion and Cracking of Plain and Reinforced Concrete Prisms due to Alkali-Silica Reaction," *ACI Materials Journal*, Vol. 95, No. 4, 1998b, 480–487.

Folliard, K.J., M. Thomas, J.A. Ideker, B. East, and B. Fournier. "Case Studies of Treating ASR-Affected Structures with Lithoum Nitrate," TRB 2009 Annual Meeting, CD-ROM, Transportation Research Board, Washington, D.C., 2009.

Folliard, K.J., R. Barborak, T. Drimalas, L. Du, S. Garber, J. Ideker, T. Ley, S. Williams, M. Juenger, M. Thomas, and B. Fournier. "Preventing ASR/DEF in New Concrete: Final Report," Technical Report No. 0-4085-5, Center for Transportation Research, The University of Texas at Austin, 2006.

Grattan-Bellew, P. E., J.J. Beaudoin, and V.G. Vallee. "Effect of Aggregate Particle Size and Composition on Expansion of Mortar Bars due to Delayed Ettringite Formation," *Cement and Concrete Research*, 28(8), 1998, 1147–1156.

Hobbs, D.W. "Expansion and Cracking in Concrete Associated with Delayed Ettringite Formation," *ACI Special Publications*, 177(11), 1999, 159–182.

Jensen, V. "Elgeseter Bridge in Trondheim Damaged by Alkali Silica Reaction: Microscopy, Expansion and Relative Humidity Measurements, Treatment with Mono-silanes and Repair," 9th Euroseminar on Microscopy Applied to Building Materials, September 9–12, 2003, Trondheim, Norway.

Kelham, S. "Effect of Cement Composition and Fineness on Expansion Associated with Delayed Ettringite Formation," *Cement & Concrete Composites*, 18(3), 1996, 171–179.

Petrov, N., M. Thibault, and A. Tagnit-Hamou. "Expansion Due to DEF in Normally Cured Concrete Heated by Cement Hydration," ACI Special Publication 234-16, American Concrete Institute, Farmington Hills, MI, 2006, 239–250.

Poole, A.B. "Introduction to Alkali-Aggregate Reaction in Concrete," *The Alkali-Silica Reaction on Concrete*, Blackie, Glasgow, Scotland, and London, Van Nostrand Reinhold, NY, 1992.

Swamy, R.N. "Testing for Alkali-Silica Reaction," *The Alkali-Silica Reaction on Concrete*, Blackie, Glasgow, Scotland, and London, Van Nostrand Reinhold, NY, 1992.

Thomas, M.D.A. “Delayed Ettringite Formation in Concrete: Recent Development and Future Directions.” *Materials Science of Concrete VI,* J. S. S. Mindess, Ed., The American Ceramic Society, Westerville, OH, 2001, 435–481.